*Original Article*

# Lung Cancer Detection Using Integration of Hybrid Segmentation Approach and DL Techniques

N. Raghapriya[1], Y. Kalpana[2]

[1,2]*Department of Computer Science, Vels Institute of Science, Technology & Advanced Studies (VISTAS), Tamil Nadu, India.*

[1]*Corresponding Author : raghapriyakamal@gmail.com*

***Abstract -*** *Cancer is a frequent illness with a rising death rate in recent years. Lung Cancer (LC) is a deadly illness that has a high patient death rate. Patients' lives can be saved by correctly determining the LC stage and receiving an early diagnosis of this illness. LC can be identified using a variety of image processing, biomarker-based, and machine automation techniques, however, medical professionals have difficulties in accurately and promptly diagnosing the disease. These automated detection systems currently use a diversity of Machine Learning (ML) methods to identify LC in its early stages. However, the processing of LC detection is time-consuming, and these systems do not offer reliable detection. This work proposes a hybrid segmentation approach that combines the Enhanced Kernal Fuzzy Clustering (EKFC) algorithm with the Global Particle Swarm Optimizer (GPSO) to carry out segmentation. CNN architecture is used to classify and extract features. The supplied image's categorization layer is responsible for identifying whether the tumor is abnormal or normal. In this work, the CT scan pictures are extracted using the lung imaging data that were acquired from the Kaggle website. The suggested segmentation methodology outperforms the other two segmentation approaches in the market with a Dice Index of 0.93. Furthermore, the Convolutional Neural Network (CNN) from the suggested segmented technique obtains 97.8% classification accuracy compared to the LSTM model.*

***Keywords*** *- CNN, CT images, Detection, EKFC, GPSO, Lung cancer.*

## 1. Introduction

Cancer is characterized by uncontrolled growth of cells, and when this uncontrolled development happens in the lungs, it is termed as LC. LC accounts for the largest portion of the many cancer deaths that occur worldwide. LC is a tumor that originates from lung cells, particularly in the epithelial lining of the bronchioles, bronchi and alveoli [1,2]. It is common and accompanied by higher death rates around the world. LC either shows no symptoms at all or mild symptoms in its early stages [2].

Consequently, it is usually detected at a later stage. Treatment effectiveness is impacted, and the chance of long-term survival is reduced when a medical issue is not detected in a timely manner [3]. Cigarette smoking is regarded as the primary cause of LC, while exposure to second-hand smoke is another significant factor. The four stages of lung carcinoma indicate the range in which the cancer has progressed throughout the body. Patients with LC only have very poor recovery rates because the disease can only be identified in its advanced stages by specialists.

The two foremost categories of LC are Small Cell LCs (SCLC) and Non-Small Cell LCs (NSCLC). The five-year endurance rate for NSCLC is 25%, while it is only 7% for SCLC. The survival rate for women is different from that of men; it is 16% for men and 23% for women. Effective screening methods are essential for the primary finding and dealing of LC in order to improve patient outcomes. Low-dose helical CT screening is superior in lowering death in high-risk groups, according to the results of the National Lung Screening Trial [4]. However, the LC screening procedure has the potential to produce False Positive (FP) results, which could cause psychological distress in patients and escalate expenditures by resulting in unnecessary medical procedures [5].

The use of CAD systems helps radiologists diagnose LC based on imaging modalities and increases patient survival rates by giving them a second opinion. Early diagnosis of LC is important for treatment planning and for increasing the patient's rate of recovery. Experts can use a variety of imaging modalities to analyse the functioning of organs and different tissues. CT image modalities are among the several that are utilized for the detection of LC because of their precision and capacity to depict body portions accurately. Early-stage LC detection can even be accomplished with CT imaging.

Determining the presence of carcinoma in CT lung images is an extremely difficult task, and identifying characteristics from the divided nodule is crucial to diagnosing

cancer in CT lung imaging. In computer vision, the technique of dividing a digital image into discrete regions or pixel groupings is called segmentation. In a particular region, every pixel shares similarity with every other pixel in at least one additional calculated property or quality, such as roughness, saturation, or color. When it comes to the same attributes, nearby locations differ substantially. Early diagnosis considerably improves both the predictive utility of the diagnosis and the capacity to plan for therapy. Since nodules are the most common sign of LC, finding them on CT scans presents a significant diagnostic problem. The hybrid Segmentation technique, which this research paper proposed, integrates one or two techniques to produce results that are more effective than segmentation algorithms working alone. GPSO is the foundation of the proposed Kernal Fuzzy clustering method. This PSO method automatically calculates the ideal number of groups. The data set is initially divided at random into a predetermined number of groups by the procedure, which then assesses the effectiveness of the clustering outcomes using a reconstruction criterion.

Deep Learning (DL) is used for classifying and recognizing LC. DL enhances the performance and accuracy of CT image recognition and categorization in addition to expediting the crucial task. CNNs are a kind of DNN that consists of many fully connected, pooling, and convolutional layers. They have shown effectiveness in the processing of images or videos, pattern recognition, and classification. In recent years, CNN has developed recognition for exceeding rivals in a number of computer vision-related applications, such as natural language processing and medical [6]. The purpose of the work is to assist in the construction of a more effective system for producing a highly accurate prediction for LC utilizing a highly efficient kernel fuzzy based global optimization algorithm based on the effective performance of DNN and CNN approaches in various image classification tasks [6, 7].

### 1.1. Research Gap

Distribution networks have made extensive use of Particle Swarm Optimization (PSO) to allocate Distribution Generators (DGs) as efficiently as possible. Nonetheless, there are certain knowledge gaps about PSO's use in this field. Improved search skills are required to prevent becoming caught in local or global optima, which is one of the gaps. The difficulty of precisely sizing and positioning DG units to reduce power losses and preserve voltage stability is another gap. The inability of current algorithms to regulate the ideal placement and size of DG units results in increased power losses. Segmentation is done using the Global Particle Swarm Optimizer (GPSO) in order to overcome these constraints. For pattern identification, one technique that is commonly employed is the Fuzzy C-Means algorithm (FCM). Its benefit is that it often produces good modelling results; nevertheless, it cannot determine the number of clusters on its own. An Enhanced Kernel Fuzzy (EKFC) is presented to optimize

FCM, based on the PSO, which is a combination of the GPSO and the EKFC technique, with the aim of addressing the issues with the FCM clustering algorithm.

Our primary contributions can be summarized as follows:
- The primary objective is to enhance patient safety by providing more accurate and superior data for medical decision-making.
- Initially, the input CT images are pre-processed using a wiener filter for the removal of noise.
- The Proposed Hybrid framework employs GPSO with EKFC for the segmentation of tumours from the abnormal CT images.
- There are three similarity index metrics used to compare the proposed segmentation method with existing methods.
- The classification of normal and abnormal CT images is done using CNN's DL methods.
- Finally, the CNN and LSTM models were used to calculate and compare statistical measures.

## 2. Literature Review

This section examines the primary clustering techniques that have been developed recently in the literature, with a specific emphasis on those that are utilized in image segmentation.

Savic, M et al. [8] examine various models of tumor segmentation. A "Single Click Ensemble Segmentation (SCES) approach" that took advantage of an execution environment was utilized for lung nodule segmentation. Essentially, the method depends on the use of several seed sites in conjunction with area growth. It employs the "Click and Grow" approach, which uses an initial seed point selected by humans to create a sector within which further kernel points are developed automatically.

Peter J. et al. [9] created a different segmentation model connected to search-based heuristics for lung tumor diagnosis. In order to separate the ROI from DICOM images, the authors first examined "PSO and genetic algorithm." They used the common "SVM algorithm" for the same in order to overcome this.

Mithoowa et al. [10] created the K-means clustering model for lung dissection. Using the "global threshold method," DICOM images are first segmented as 2D, and then the author assesses the presence or absence of lung cancers. The K-means model's drawback is that it can only segment nodules in the lungs larger than 7 mm in diameter.

In order to identify pulmonary nodules in LC diagnosis, Monica Ramakrishnan et al. [11] created a method to detect LC nodules using CT scans in 2022. This method offers CNN implementation using the RNN as classification and the pre-trained VGG model for acquiring features.

Radhanadh Patra et al. [12] presented a KNN, ML, and RBF-based LC prediction algorithm. A number of ML classifier techniques were employed to classify as benign or malignant the publicly accessible LC data in the UCI ML repository. The Weka tool uses a number of widely recognized classifiers to classify the data collection as either normal or abnormal after first obtaining the input and converting it to binary.

Md. Rashidul Hasan et al. [13] suggested image processing and statistical learning for LC classification and detection. GLCM was used to extract the data in this instance, which involved applying a genetic method to identify particular traits. LC stages were categorized using SVM. An algorithm has been developed to ascertain whether lung abnormalities are normal or abnormal accurately.

Dhanush Raj et al. [14] describe a strategy for identifying LC using different image-processing techniques. The method that is most frequently employed is CT image processing. In this method, the issues related to LC detection have been addressed. CT scans of the lungs are the input datasets in this instance. The initial step involves enhancing the image through the utilization of retrieved CT pictures. In the subsequent phase, the enhanced image undergoes segmentation. When segmenting images, the watershed approach is employed, and it is highly susceptible to local minima. When segmenting images, the watershed approach is employed, and it is highly susceptible to local minima.

Aghamohammadi et al. [15] discuss segmentation, which involves dividing regions in images into numerous coherent sub-regions by leveraging statistical features like texture and colour. This also includes classifying each grouped sub-region based on pixels. Recently, there has been considerable progress in the development of CAD tools aimed at enhancing cancer diagnosis through more precise segmentation techniques.

Ghoushchi et al. [16] have shown that these methods typically enhance the tumor detection rate. Specifically, advancements in machine learning have influenced the medical domain and are increasingly being incorporated into CAD systems.

Khairandish et al. [17] introduced a model where they categorized tumors into malignant and benign classes. Additionally, they employed a threshold-based system to identify brain tumors. In their investigation, they did not specifically address ROI segmentation.

Z. Yang [18] introduced a shallow CNN for both classification and segmentation tasks using stool medical images. They classified the colour of the faeces by first segmenting the effective region of stools and then using a categorizing level. Their technique produced accurate colour classification and low-cost automatic segmentation.

Y. Yang [19] introduced a Mask-Refined R-CNN (MRR-CNN) model. Their model was simple to use and time-efficient.

Liu et al. [20] developed a feature fusion module using an attention-based modality selection approach to handle the differences between various modalities for a particular segmentation target.

Afridi et al. [21] examine supervised and statistical machine learning techniques; users are still required to identify the features on their own. It is a challenging task, and experience is needed. Convolutional approaches, on the other hand, are a prominent DL technique that allows for the automatic extraction of features. Because of this, in addition to machine learning, researchers are now using DL-based brain tumour segmentation. Batch-based classification is a common approach used in DL-based systems.

S. Sasikala et al. [22] identify and categorize LC from CT scan images. They conducted two phases of training, the first was classification, and the second was the usage of MATLAB to extract valuable volumetric information from the input data. Their suggested method has a 96% classification accuracy for malignant and non-cancerous cells.

SRS Chakravarthy et al. [23] implemented a Probabilistic Neural Network (PNN) for the classification job and utilized the Gray Level Co-Occurrence Matrix (GLCM) and Chaotic Crow Search Algorithm (CCSA) for feature selection on CT. They discovered that, with 90% accuracy, the PNN model based on CCSA characteristics worked better.

M. Saric et al. [24] developed using whole-side histopathology pictures for LC identification. These designs implemented VGG and ResNet. ROC plot was used to compare the output of the CNN architectures. Patch level performance for ResNet50 and VGG16 was found to be 0.7541 and 0.7205, respectively. These are extremely low values. Through a number of slides, they clarified that the high pattern diversity was the cause of the models' poor accuracy.

## 3. Dataset Description
The datasets that were used to obtained from the Kaggle website. These datasets included 2,351 different types of X-ray and CT scan images, totaling about 70.125 GB. Both normal and pathological lung images were included in the data sets used in this investigation. There are 572 images of aberrant lung images and 325 images of normal lung images. JPEG format is used for the images.

### 3.1. Data Preprocessing
The noise in CT lung images must be eliminated in order to increase the precision of the system that recognizes and categorizes abnormalities in CT lung images. In order to

improve the clarity of the CT lung images by removing noise from the data, filters are applied during pre-processing. In the present study, noise is eliminated by the application of Wiener filters. Equation (1) provides an optimal description of the wiener filter, which was designed based on the stochastic structure.

$$w(f1, f2) = \frac{H*(f1,f2)S_{xx}}{|H(f1,f2)|^2 S_{xx}(f1,f2)+S_{\eta\eta}(f1,f2)} \quad (1)$$

Where the noise and the power spectrum of the CT image are embodied by $S_{xx}(f_1, f_2)$, $H(f_1, f_2)$ and $S_{\eta\eta}(f_1, f_2)$, which are the blurring filter. The Wiener filter holds the edges and eliminates noise by using inverse and low-pass filters.

# 4. Research Methodology

In order to increase the fitness value of every particle, a novel GPSO and KFCM algorithm has been proposed in this study effort and applied to each particle for an infinite number of iterations.

## 4.1. GPSO Segmentation Algorithm

The main focus of this algorithm is that new particles deal with the current best location in the neighbourhood. The existing canonical PSO algorithm cycles through equations (2) and (3), one of which determines the particle's position and the other of which determines its velocity.

$$u_i = wu_i(t) + a_1 r_1 \big(P_i - y(t)\big) + a_2 r_2 \Big(P_g - y_i(t)\Big) \quad (2)$$

$$y_i(t+1) = y_i(t) + u(t) \quad (3)$$

Where $u_i$ (t) and $y_i$ (t) are vectors indicating the present location and velocity correspondingly, $0 \leq W < 1$ is a weight of inertia that controls the amount of the initial velocity particle that is retained, $a_1$ and $a_2$ are two variables of constructive velocity, $r_1$ and $r_2$ are two identical combinations of random events were taken from U (0,1), $P_i$ represents best position of the particle-initiate by the $i^{th}$ particle and $P_g$ represents finest location so far discovered by the entire swarm.

Equation (4) can be created by combining the updated Equations (2) and (3), assuming equal zero.

$$y_i(t+1) = y_i(t) + a_1 r_1 \big(P_i - y_i(t)\big) + a_2 r_2 \Big(P_g - y_i(t)\Big) \quad (4)$$

The local search capability is increased, while this formula decreases the global search capability. So, if $y_j$ (t) = $P_j = P_g$, particle j at the velocity zero. In order to increase the

swarm's $P_g$ current best position, we conserve it. Also arbitrarily initialize particle j's position $y_j$ (t + 1), and modify the other particles in accordance with equation (4), which results in equation (5).

$$P_j = y_j(t+1) \quad (5)$$

If $P_j = P_g$, then the particle j's position $y_j$ (t + 1)must continue to randomly initialize and manage additional particles in accordance with (5); if $P_j = P_g$, and remains constant, all particles are controlled in accordance with (5); if $P_j = P_g$, and changes $p_g$, an integer k1j exists, which is satisfied using $y_k$ (t + 1)= $P_k = P_g$, therefore, in accordance with Equation (5), the position of particle k represents $y_k$ (t) must continue to be initialized arbitrarily, and other particles are changed thus the improved global search capability. The enhanced PSO technique known as Global PSO (GPSO) is required due to the particle's position needing to be consistently selected from the domain when $y_j$ (t) = $P_j$.

## 4.2. EKFC Segmentation Algorithm

It is the process of breaking up an image into distinct areas that share similar characteristics. In this case, each pixel in the EKFC algorithm is given a unique membership value, which combines the clusters that have formed in the image space. Equation (6) represents the general equation or objective function of EKFC.

$$J_{KFCM} = \sum_{I=1}^{M} \sum_{j=1}^{c} v_{ij}^n \, ||P_i - Q_j||^2, 1 \leq n < \infty \quad (6)$$

Where m is the regularisation exponent to the fuzziness level,n> 1, and $||P_i - Q_j||^2$ is the distance between i and $Q_j$ in grayscale Euclidean distance in Equation (7).

$$\sum_{j=1}^{c} v_{ij} = 1, v_{ij} \in [0,1], 0 \leq \sum_{i=1}^{M} v_{ij} \leq M \quad (7)$$

Equations (8) and (9) are used to iteratively update the cluster centres using the membership function from the alternate optimisation.

$$v_{ij} = \frac{1}{\sum_{k=1}^{c}(||P_i - Q_j||^2/||P_i - Q_k||^2)^{1/(n-1)}} \quad (8)$$

$$Q_j = \frac{\sum_{i=1}^{M} v_{ij}^n P_i}{\sum_{i=1}^{M} v_{ij}^n} \quad (9)$$

This study proposes a modified EKFC, where C is a correlation function or correlation distance measure. Finding the ideal value $\eta_j$ necessitates a large number of cluster

centres in addition to a large number of patterns for the general identification of C. Equation (10) shows how a fuzzy factor is used to combine scale and geographical context information in order to solve this issue.

$$J_{C-KFCM} = \sum_{i=1}^{M} \sum_{j=1}^{c} [v|ij^n||P_i - Q_j||^2 + F_{ij}] \quad (10)$$

With this modified fuzzy, the correlation function takes the place of the distance and governs the local neighbor relationship. The fuzzy factor i is represented by $w_{ik}$, and the correlation metric function is represented by $1 - C(P_i, Q_j)$.

### 4.3. The Proposed Hybrid Segmentation GPSO with EKFC Algorithm

The new particle deals with the current best position in the neighborhood and is the main focus of the GPSO - EKFC algorithm. Equation (11) presents a new particle for the velocity update equation, wherein every element is regarded as a member of the swarm in the present research.

$$u\varphi(t+1) = y\varphi(t) + Pbest(t) + Wu\varphi(t) + P(t)(1-2r) \quad (11)$$

The area of the best position was enhanced to make a better random search. The random diameter r and φ(t) represent the random search region of the random vector. FCM is a clustering technique that supports dividing into several clusters. Equation (8) is used to iteratively update the cluster center's upgrade function and minimize the goal function in Equation (6).

At last, determine the global best position (Gbest) for the swarm and the best position (Pbest) for the total particle population. In FCM, the GOTO first stage is triggered if KFC is the termination state; if the GPSO terminating state is not satisfied, the method's GOTO initial stage is triggered. The hybrid segmentation methodology that combines GPSO and EKFC was examined in this study and was determined to be the more efficient approach.

### Algorithm of GPSO – EKFC
**Input:** Number of clusters (C), fuzzification coefficient (M), and data set Y = [y1, y2,...,yn].
**Output:** The partition matrix U of size n × c and its matching center
Step 1: Initialize a swarm at random
Step 2: The iteration begins with t=1.
Step 3: The velocity for every particle needs to be updated using equation 4.
Step 4: The location of each particle is updated using Equation 5.
Step 5: Utilizing equation 11, update the individual and global best scores.
Step 6: Determine the partition matrix U.
Step 7: Proceed to Step 3. If the stoppage requirement is not

satisfied, then t = t +1.
Step 8: Use the partition matrix U of the Gbest to replicate the original data.
Step 9: The Reconstruction Criterion (RC) is applied in order to assess the eight distinct indices consistently. The original data vectors are "reconstructed" according to the reconstruction criterion using the partition matrix and cluster prototypes. Equation 9 computes the rebuilt form of the original data vectors.
Step 10: When the reconstruction is finished, the squared error of the original vectors and the reconstruction vectors is estimated using Equation 6.
Step 11: Choose the centers and partition matrix that result in the least amount of reconstruction error.

### 4.4. Feature Extraction (FE) and Classification of LC Using CNN

FE is the process of identifying the characteristics of the objects in the image. Another way to define FE is as the process of taking raw data and turning it into accessible numerical characteristics while keeping the initial data's essence. The procedure of FE is necessary to illustrate the result and establish whether an image is abnormal or normal. The categorization process is based on these features. To enhance identification accuracy, these undesirable regions need to be eliminated. Since binary images can exist without colour. To locate lung cancers, dimension and shape parameters such as region, major and minor axis, and firmness were evaluated. The average level of intensity, area, circumference, and eccentricity were the only features that were believed to be retrievable.

The exact outline number of the nodular pixel, denoted by the scalar value, is obtained by adding the associated outlines of each recognized pixel in the binary image.

CNN is utilized in patient CT images to identify and classify LC. Neural Networks (NN) have a subtype called CNNs. NN is designed to resemble the way of brain functions and learns. It passes information across several layers in order to receive it, process it, and produce an output. The output layer is on the right side, and the input layer is on the left. Since the values of these levels are not immediately visible in the training set, the middle layers—also known as hidden layers—are where the "magic" happens. The deeper a network gets, the greater the number of hidden layers there are separating the input and output levels.

Every sort of layer may occur multiple times. The sequence of the layers is unspecified but follows certain guidelines.

The objective of CNNs is to transform images into a comprehensible format, preserving crucial elements necessary for precise predictions. Within the middle layer are pooling, convolutional, fully connected, ReLU and other layers. Using

these layers, the CNN was constructed. Figure 1 depicts the CNN layers.

The CT images from this input layer are passed to additional layers for FE. This layer includes all the filters that are applied to images in order to obtain features. These attributes are used to establish matches during the testing stage. The filter size (F) and kernel dimension (K) of the convolutional layers in the first region are 3×3 and 128×128 correspondingly. The convolutional layers in the second level have 256×256 number of filter and the same 3×3 size of filter as those in the first levels. CNN architecture blocks 1 through 2's max-pooling layers applied the 2×2 and 3×3 interleaved sequence. The convolutional-pooling layer blocks are employed to extract features from input. Table 1 displays the values of hyperparameters taken into consideration for the CNN architecture in this work.

**Table 1. Model description**

| S.no | Specification | Hyperparameter Values |
|------|---------------|------------------------|
| 1 | Batch quantity | 128 |
| 2 | Pooling stages | 02 [(2,2), (2,2)] |
| 3 | Filter dimension | [(3,3)] |
| 4 | Padding | Zero padding, (1,1) padding |
| 5 | Training Dataset | 70% (from data pre-processing) |
| 6 | Fall – off rate | 0.2 |
| 7 | Kernel dimension | [(128,128), (256,256)] |
| 8 | Testing Dataset | 30% (from data pre-processing) |
| 9 | Epoch count | 05 |
| 11 | Stride Size | (1,1) |
| 12 | Convolutional levels | 02[1conv – 1conv] |

A filter that predicts the class probabilities for each feature by scanning the entire image a few pixels at a time produces a feature map. Following that, data is sent to the pooling layer, which keeps the most important information while reducing the amount of data generated by the convolutional layer for each feature (the operations of the pooling and convolutional layers are usually done several times). Next, the fully connected layer is substantially used. In order to forecast a suitable layer. The result of the feature analysis weights is applied to the pattern analysis input to get the final categorization possibilities for the image, which are then used to forecast an appropriate label. Equations 12 and 13 can be used to determine feature map dimensions.

$$H_o = \frac{H_i - Fh + 2p}{s} + 1 \qquad (12)$$

$$W_o = \frac{W_i - Fw + 2p}{s} + 1 \qquad (13)$$

Fully connected layer $w = (n + 1) * m$

Which 'n' represents inputs to the layer and 'm' represents output nodes. CNN is a type of DL model designed to analyse images by utilizing adjustable weights and biases to discern various elements within the image. Figure 1 illustrates the specific architecture employed for diagnosing LC using CNN technology.

# 5. Results and Discussion

The proposed approach was validated, and its functionality and results were tested using a series of simulated evaluation studies. MATLAB has built-in tools for image processing, it was essential to use it in all simulated scenarios. The original LC CT picture, the segmented PSO output, the segmented Fuzzy C Means clustering output, and the suggested GPSO-EKFC algorithm are all shown in Table 2.

The performance of the segmentation method is determined by comparing the proposed segmentation image with the aforementioned segmentation methods based on ground truth image using the Jaccard Index (JI), Hammoude Index (HM) and Dice Index (DI) to estimate how well the segmentation methods performed.

## 5.1. Jaccard Index (JI)

The JI is a statistic used to assess how similar and diverse two data frames are. The data windows Xi and Xj should be considered. The coefficient, which evaluates the level of overlap between the two windows, is calculated from the ratio of common qualities between windows Xi and Xj.

For simplicity, disregard data windows in favour of two sets, A and B. The region of intersection (A ∩ B) and union (A ∪ B) between these two sets can be measured thanks to set theory. As a result, equation 14 uses the following formula to determine the Jaccard index.

$$\text{Jaccard (A, B)} = \frac{A \cap B}{A \cup B} \qquad (14)$$

## 5.2. Dice Index (DI)

Equation 15 defines the conventional Dice coefficient.

$$DI = \frac{2\,|A \cap B\,|}{|\,A|+|B|} \qquad (15)$$

Here, A is a set reflecting the actual data, and B is the segmentation that was generated segmentation. Each voxel in both images (sets) has a binary value of '0' or '1'. (or pixels in the 2D case). Here, a and b are used to represent these values, respectively.
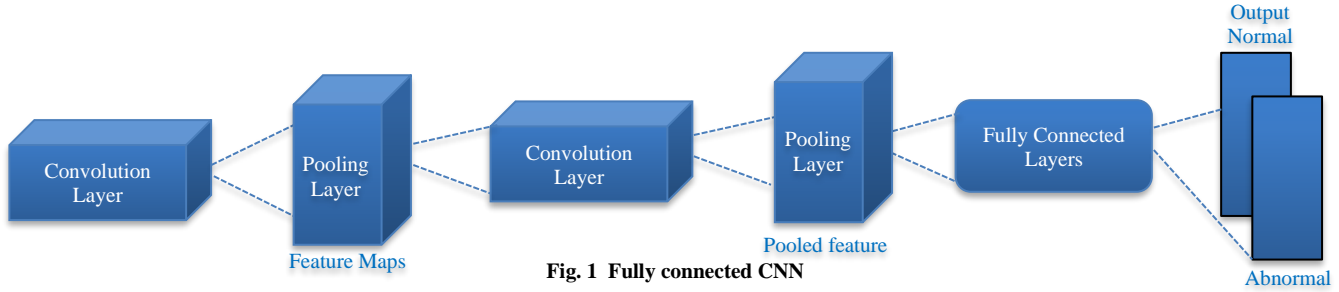
**Fig. 1 Fully connected CNN**

### 5.3. Hammoude Index (HM)

It makes a pixel-by-pixel comparison enclosed by the two boundaries defined in Equation 16.

$$HM\ (A,\ B) = \frac{(A\ U\ B) - (A\ \cap B)}{(A\ \cup B)} \qquad (16)$$

Table 2 shows the comparison of normalized mean values based on validating parameters for the proposed GPSO-EKFC algorithm with the existing PSO and Fuzzy C means algorithm. The closer the segmented image contour is to the highest-quality image contour, the bigger the values of the JI and DI, which are closer to one. The segmented image contour is more similar to the highest-quality image contour when the HI is low (around zero). Table 3 shows the final result of segmented lung CT.

**Table 2. Validating parameters for proposed GPSO-EKFC with existing methods**

| Segmentation algorithm | JI | DI | HI |
|---|---|---|---|
| PSO | 0.85 | 0.91 | 0.19 |
| Fuzzy C-Means | 0.81 | 0.9 | 0.22 |
| Proposed GPSO-EKFC | 0.87 | 0.93 | 0.14 |

**Table 3. Overall comparison of segmented lung CT image**

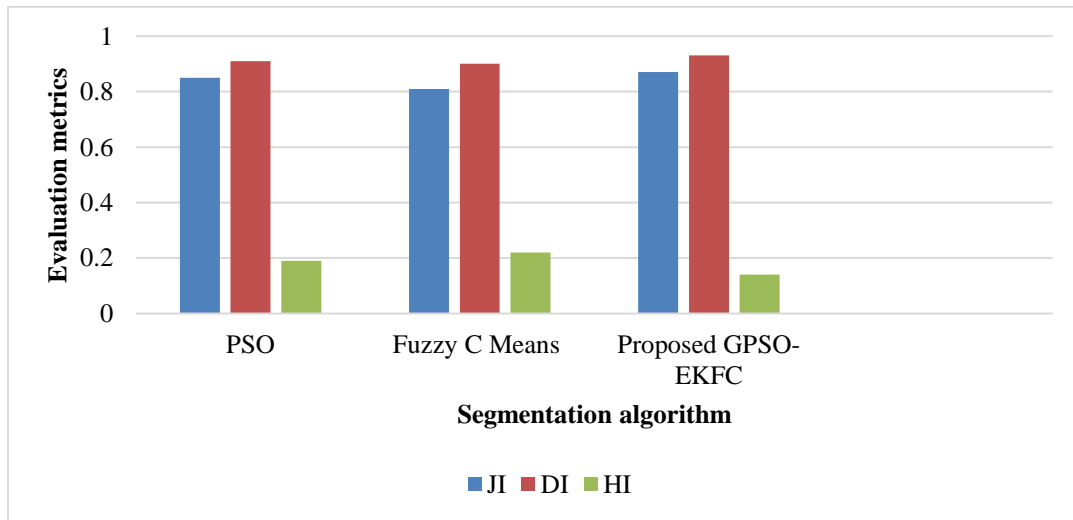| Input image | PSO algorithm | Fuzzy C means clustering | Proposed GPSO-EKFC algorithm |
|---|---|---|---|





**Fig. 2 Comparative results of the performance evaluation metrics of the proposed algorithm with the existing algorithm**

Figure 2 shows comparative evaluation metrics of the proposed GPSO-EKFC, PSO and Fuzzy C Means algorithm. According to the outcomes, the proposed GPSO-EKFC segmentation approach outperforms the other two methods.

This paper presented a unique DL-based method to identify and categorize LC on CT scans. DL can autonomously identify significant features without requiring human intervention. This is especially helpful for tasks like picture categorization that have hard-to-define properties. Large and complex datasets can be handled using these techniques. In this work, CNN is utilized for FE and categorization. Based on the features acquired, the CNN classification establishes whether the lung tumor was aberrant (lung tumor was impacted) or normal (lung tumor was not affected). The 80:20 ratios of the LC images are segregated for training and testing.

Lastly, the CNN model assesses a wide range of performance metrics in order to contrast itself with alternative LSTM models. The following parameters are computed: 1. True Positive (TP): represents the number of types in the dataset that have been sufficiently identified; 2. False Positive (FP): counts the number of incorrectly predicted kinds; 3. True Negative (TN): indicates the quantity of sound lungs that were accurately recognized; 4. False Negative (FN): counts the quantity of negative samples that were mistakenly detected; Table 4 illustrates the Confusion Matrix (CM) for the DL model that makes use of the suggested segmentation procedure.

**Table 4. CM for CNN and LSTM model based on suggested GPSO-EKFC algorithm**

| Model Description | TP | TN | FP | FN | TP |
|---|---|---|---|---|---|
| CNN | 140 | 79 | 3 | 2 | 140 |
| LSTM | 135 | 80 | 3 | 6 | 135 |

Table 5 demonstrates how the accuracy, recall, sensitivity, F1 score, specificity, and precision of binary class classification may be evaluated using the FP and FN examples.

Sensitivity: The classifier properly identifies the proportion of positive values.

$$Sensitivity = \frac{TP}{TP+FN}$$

Specificity: The percentage of negative values is inaccurately identified by the classifier.

$$Specificity = \frac{TN}{TN+FP}$$

Accuracy: Calculate the percent of accurately identified instances to the entire number of test cases using the formula below.

$$Accuracy = \frac{TP+TN}{TP+TN+FP+FN}$$

Precision: the ratio of the identified types over the total of the mistakenly identified classes plus the real classes that are categorized correctly.

$$Precision = \frac{TP}{TP+FP}$$

Recall: The true positive rate indicates the number of accurate positives detected and classified by the model.

$$Recall = \frac{TP}{TP+FN}$$

$$F1 = 2 \times \frac{Precision \times Recall}{Precision+Recall}$$

**Table 5. The performance evaluation of the segmentation algorithm for the detection of LC**

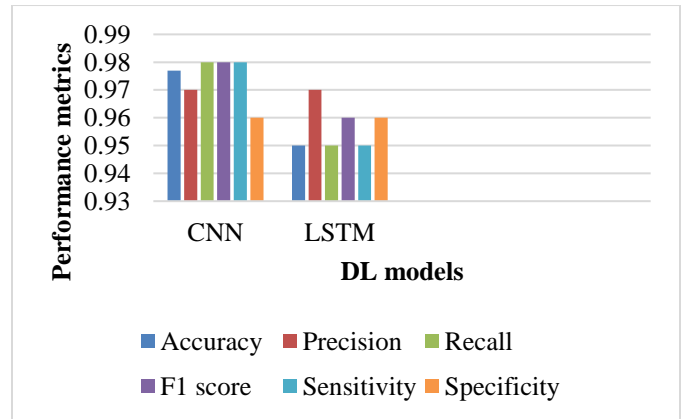| Model Description | Accuracy | Precision | Recall | F1 score | Sensitivity | Specificity |
|---|---|---|---|---|---|---|
| CNN | 0.977 | 0.97 | 0.98 | 0.98 | 0.98 | 0.96 |
| LSTM | 0.95 | 0.97 | 0.95 | 0.96 | 0.95 | 0.96 |



**Fig. 3 Performance evaluation of DL models based proposed GPSO-EKFC segmentation algorithm**

The accuracy score for CNN is 0.97, which illustrates the detection of LC as the most accurate when compared with the LSTM model, as shown in Figure 3.

## 6. Conclusion

The proposed method determines and controls the ideal number of clusters by combining GPSO and EKFC with a threshold vector. Through an iterative fuzzy partitioning method, the algorithm resolves the clustering issue. The GPSO, which is based on the gradient descent of EKFC in feature space, takes the role of the iteration process, giving the algorithm a strong global searching capability and avoiding

EKFC's local minimum issues. Meanwhile, there is less of a reliance on the initialization values for FCM. Simulation trials validate the algorithm's efficiency and viability. This study uses a combination of suggested segmentation techniques and DL to separate tumors from CT lung images. The framework's classification of aberrant and normal lung images is the most crucial phase. The CNN classification helps to lower the number of false positives. When compared to LSTM, the suggested system-based CNN model performs better, delivering 97% accuracy and reducing false positives. Additionally, the system's decision-making is accurate when compared to that of a human doctor. We intend to employ a variety of feature selection techniques in the future and determine which feature selection technique provides the best efficiency and accuracy for tumor segmentation and classification.

## References

[1]  Yu Gu et al., "A Survey of Computer-Aided Diagnosis of Lung Nodules from CT Scans using DL," *Computers in Biology and Medicine,* vol. 137, 2021. [CrossRef] [Google Scholar] [Publisher Link]

[2]  Muhammad Irfan Sharif et al., "A Comprehensive Review on Multi-Organs Tumor Detection Based on Machine Learning," *Pattern Recognition Letters,* vol. 131, pp. 30–37, 2020. [CrossRef] [Google Scholar] [Publisher Link]

[3]  Thamali Madhushani Adhikari et al., "A Review of Deep Learning Techniques Applied in Lung Cancer Diagnosis," *Signal and Information Processing, Networking and Computers, Proceedings of the 6th International Conference on Signal and Information Processing, Networking and Computers,* Guiyang, China, pp. 800–807, 2020. [CrossRef] [Google Scholar] [Publisher Link]

[4]  A. Asuntha, and Andy Srinivasan, "Deep Learning for Lung Cancer Detection and Classification," *Multimedia Tools and Applications,* vol. 79, pp. 7731–7762, 2020. [CrossRef] [Google Scholar] [Publisher Link]

[5]  P. Mohamed Shakeel, M.A. Burhanuddin, and Mohamad Ishak Des, "Lung Cancer Detection from CT Image Using Improved Profuse Clustering and Deep Learning Instantaneously Trained Neural Networks," *Measurement,* vol. 145, pp. 702–712, 2019. [CrossRef] [Google Scholar] [Publisher Link]

[6]  D. Jude Hemanth, Omer Deperlioglu, and Utku Kose, "An Enhanced Diabetic Retinopathy Detection and Classification Approach Using Deep Convolutional Neural Network," *Neural Computing and Applications,* vol. 32, pp. 707–721, 2020. [CrossRef] [Google Scholar] [Publisher Link]

[7]  Arun Singh Yadav et al., "A Feature Extraction using Probabilistic Neural Network and BTFSC-Net Model with DL for Brain Tumor Classification," *Journal of Imaging*, vol. 9, no. 1, pp. 1-22, 2023. [CrossRef] [Google Scholar] [Publisher Link]

[8]  Marko Savic et al., "Lung Nodule Segmentation with a Region-Based Fast Marching Method," *Sensors*, vol. 21, no. 5, pp. 1-32, 2021. [CrossRef] [Google Scholar] [Publisher Link]

[9]  Peter J. Mazzone et al., "Screening for Lung Cancer, CHEST Guideline and Expert Panel Report," *Thoracic Oncology: Guideline and Consensus Statement,* vol. 160, no. 5, pp. e427-e494, 2021. [CrossRef] [Google Scholar] [Publisher Link]

[10] Hamid Mithoowani, and Michela Febbraro, "Non-Small-Cell Lung Cancer in 2022: A Review for General Practitioners in Oncology," *Current Oncology,* vol. 29, no. 3, pp. 1828-1839, 2022. [CrossRef] [Google Scholar] [Publisher Link]

[11] Monica Ramakrishnan et al., "*Automated Lung Cancer Nodule Detection,*" Thesis, Santa Clara University, pp 1–37, 2022. [Publisher Link]

[12] Radhanath Patra, "Prediction of Lung Cancer using Machine Learning Classifier," *Computer Science, Communication and Security,* pp. 132–142, 2020. [CrossRef] [Google Scholar] [Publisher Link]

[13] Md Rashidul Hasan, and Muntasir Al Kabir, "Lung Cancer Detection and Classification based on Image Processing and Statistical Learning," *Journal of Emerging Trends in Engineering and Applied Sciences,* vol. 11, no. 6, pp. 229-236, 2020. [Google Scholar] [Publisher Link]

[14] Raj D, Rekha BS, "Detection and Classification of LC Using Image Processing Technique," J Emerg Technol Innov Res, vol. 6, no. 5, 2019.

[15] Amirhossein Aghamohammadi et al., "TPCNN: Two-Path Convolutional Neural Network for Tumor and Liver Segmentation in CT Images Using a Novel Encoding Approach," *Expert Systems with Applications,* vol. 183, 2021. [CrossRef] [Google Scholar] [Publisher Link]

[16] Saeid Jafarzadeh Ghoushchi et al., "An Extended Approach to Predict Retinopathy in Diabetic Patients Using the Genetic Algorithm and Fuzzy C-Means," *BioMed Research Internatioal,* pp. 1-13, 2021. [CrossRef] [Google Scholar] [Publisher Link]

[17] M.O. Khairandish et al., "A Hybrid CNN-SVM Threshold Segmentation Approach for Tumor Detection and Classification of MRI Brain Images," *IRBM*, vol. 43, pp. 290–299, 2022. [CrossRef] [Google Scholar] [Publisher Link]

[18] Ziyuan Yang, Lu Leng, and Byung-Gyu Kim, "StoolNet for Color Classification of Stool Medical Images," *Electronics,* vol. 8, no. 12, pp. 1–15, 2019. [CrossRef] [Google Scholar] [Publisher Link]

[19] Yiqing Zhang et al., "Mask-Refined R-CNN: A Network for Refining Object Details In Instance Segmentation," *Sensors,* vol. 20, no. 4, pp. 1–16, 2020. [CrossRef] [Google Scholar] [Publisher Link]

[20] Yu Liu et al., "Brain Tumor Segmentation in Multimodal MRI via Pixel-Level and Feature-Level Image Fusion," *Frontiers in Neuroscience,* vol. 16, pp. 1-15, 2022. [CrossRef] [Google Scholar] [Publisher Link]

[21] Muhammad Afridi et al., "Brain Tumor Imaging: Applications of Artificial Intelligence," *Seminars in Ultrasound, CT and MRI,* vol. 43, pp. 153–169, 2022. [CrossRef] [Google Scholar] [Publisher Link]

[22] S. Sasikala, M. Bharathi, and B.R. Sowmiya, "Lung Cancer Detection and Classification Using Deep CNN," *International Journal of Innovative Technology and Exploring Engineering,* vol. 8, no. 2S, pp. 259-262, 2019. [Google Scholar] [Publisher Link]

[23] S.R. Sannasi Chakravarthy, and Harikumar Rajaguru, "Lung Cancer Detection using Probabilistic Neural Network with modified Crow-Search Algorithm," *Asian Pacific Journal of Cancer Prevention,* vol. 20, no. 7, pp. 2159-2166, 2019. [CrossRef] [Google Scholar] [Publisher Link]

[24] Matko Šarić et al., "CNN-based Method for LC Detection in Whole Slide Histopathology Images," *4ᵗʰ International Conference on Smart and Sustainable Technologies (SpliTech),* Split, Croatia, pp. 1-4, 2019. [CrossRef] [Google Scholar] [Publisher Link]